CALCULATED INTERDIFFUSIVITIES RESULTING FROM DIFFERENT FITTING FUNCTIONS APPLIED TO MEASURED CONCENTRATION PROFILES IN Cu-RICH FCC Cu–Ni–Sn ALLOYS AT 1073 K

Y. Liu [a], D. Liu [b], Y. Du [a, *], S. Liu [a], D. Kuang [c], P. Deng [a], J. Zhang [a], C. Du [d], Z. Zheng [d], X. He [e]

[a] State Key Laboratory of Powder Metallurgy, Central South University, Changsha, Hunan, China
[b] Institute of Electrical Engineering, Chinese Academy of Sciences, Beijing, China
[c] Shenzhen Technology University, Shenzhen, Guangdong, China
[d] School of Mathematics and Statistics, Central South University, Changsha, Hunan, China
[e] Insititute of Materials, Chinese Academy of Engineering Physics, Mianyang, Sichuang, China

Abstract

Employing six groups of bulk diffusion couples together with electron probe microanalysis technique, the composition-dependences of ternary interdiffusion coefficients in Cu-rich fcc Cu–Ni–Sn alloys at 1073 K were determined via the Whittle and Green method. Different fitting functions applied to the measured concentration profiles are utilized to extract the interdiffusion coefficients of fcc Cu–Ni–Sn alloys. The errors for the obtained interdiffusivities are evaluated by a scientific method considering the error propagation. The calculated diffusion coefficients using the Boltzmann and additive Boltzmann functions are found to be with reasonable errors and show a general agreement with those using other fitting functions. Based on the Boltzmann and additive Boltzmann functions, the interdiffusivities in Cu-rich fcc Cu–Ni–Sn alloys at 1073 K are obtained and validated by thermodynamic constraints. The Boltzmann and additive Boltzmann functions are recommended to be used for the fitting of measured concentration profiles in other ternary systems for the sake of extracting ternary diffusivities.

Keywords: Ternary diffusivities; fcc Cu–Ni–Sn alloys; Diffusion couples; Fitting functions; Concentration profile.

1. Introduction

As a high strength and high elasticity copper-based materials, Cu–Ni–Sn alloys have wide applications also owing to their high thermal and electrical conductivity, good mechanical, physical and corrosion resistance properties [1-3]. Furthermore, Sn-based alloys are promising and potential candidates for Pb-free solders and the interfacial reactions between solder alloys and metal substrates containing Cu and Ni are of great concern [4-6]. The comprehensive understanding of the diffusion behavior is essential to investigate and optimize the performance of such alloys, since the microstructure evolution is largely dependent on diffusion [7]. The strength and elasticity of Cu–Ni–Sn alloy can be markedly changed by heat treatment, which is critically controlled by diffusion [2]. Besides, the diffusion behavior among Cu, Ni and Sn elements has a significant influence on the reliability of the solder

joints and then on the mechanical and electrical properties of the electronic devices [8]. Therefore, it is highly desirable to investigate the diffusion behavior in the Cu–Ni–Sn system.

However, there is still no any experimental study of diffusivity in fcc Cu–Ni–Sn system in the literature. Hence, one of the main objective in the present work is to investigate the interdiffusivities in Cu-rich fcc Cu–Ni–Sn alloys at 1073 K. The single-phase diffusion couple technique with Whittle and Green method is a traditional and reliable way to determine the interdiffusivities of the target phase [9-11]. It is generally believed that one can only measure an accurate diffusivity at an intersection point of two diffusion couples [12]. In this study, the interdiffusion profile has been acquired by means of electron probe microanalysis (EPMA) and the experimental part shall be displayed in next Section. Due to the scattered and limited original data in the measurement of EPMA, the fitting functions applied to the measured

---

Dedicated to the memory of Professor Dragana Živković

concentration profiles are proposed. Therefore, the other main purpose is to analyze the effect of different fitting functions and choose the more suitable one for the determination of ternary diffusivities of fcc Cu–Ni–Sn alloys according to the scientific error propagation method. The method of evaluating ternary interdiffusion coefficients will be presented in Section 3. Section 4 is going to investigate different fitting functions applied to measured concentration profiles and obtain the interdiffusivities in Cu-rich fcc Cu–Ni–Sn alloys at 1073 K. Then the main conclusions will be presented in the last Section.

2. Experimental procedure

Six Cu–Ni–Sn diffusion couples were designed and their terminal compositions are listed in Table 1. Binary/ternary alloys with terminal compositions were prepared firstly using copper (purity: 99.99 wt.%), nickel (purity: 99.99 wt.%) and tin (purity: 99.99 wt.%) as starting materials. These alloys were prepared by arc melting under an argon atmosphere using a non-reactive W electrode (WKDHL-1, Optoelectronics Co. Ltd., Beijing, China). All the buttons were re-melted five times to guarantee their homogeneity and the total weight losses after preparation were less than 1 wt.%. Subsequently, the samples were linearly cut into blocks of approximate dimensions $5 \times 5 \times 10$ mm³ before mechanically removing the surface material. Then these blocks were sealed into an evacuated quartz tubes, and homogenized at 1073 ± 5 K for 45 days in an L4514-type diffusion furnace (Qingdao Instrument & Equipment Co., Ltd., China), followed by quenching in water. The polished and cleaned blocks were bounded together by molybdenum wires to form diffusion couples according to the assembly listed in Table 1. These couples were then sealed into quartz tubes and annealed at 1073 K for 36 h followed by quenching in water. After standard metallographic technique, the concentration profiles of each diffusion couple were determined by EPMA (JXA-8230, JEOL, Japan). Variations in alloy compositions were determined to be within ± 0.5 at.% for each component.

Table 1. List of terminal compositions of the diffusion couples in the present work.

Couple	Composition (at.%)
C1	Cu–6.95Ni/Cu–4.58Sn
C2	Cu–3.48Ni/Cu–4.49Sn
C3	Cu–7.14Ni/Cu–2.31Sn
C4	Cu–3.54Ni/Cu–2.25Sn
C5	Cu/Cu–4.06Ni–2.83Sn
C6	Cu/Cu–9.11Ni–1.40Sn

3. Methods for evaluating ternary interdiffusion coefficients

The concentration profiles for diffusion couples are analyzed by means of the Whittle–Green method [13] to obtain the ternary interdiffusion coefficients in the fcc Cu–Ni–Sn alloys. Taking component 3 as the solvent, the interdiffusion in a hypothetical 1–2–3 ternary system can be expressed by an extended Fick's second law on the basis of Matano coordinates:

$$\frac{\partial C_i}{\partial t} = \frac{\partial}{\partial x}(\tilde{D}_{i1}^3 \frac{\partial C_1}{\partial x}) + \frac{\partial}{\partial x}(\tilde{D}_{i2}^3 \frac{\partial C_2}{\partial x}) \ (i=1,2) \qquad (1)$$

where x is the distance, t represents time and C_i is concentration of component i. The main interdiffusion coefficients, $\tilde{D}_{11}^3$ and $\tilde{D}_{22}^3$, represent the influences of the concentration gradients of elements 1 and 2 on their own fluxes, respectively. $\tilde{D}_{12}^3$ and $\tilde{D}_{21}^3$ are the cross interdiffusion coefficients which represent the influences of the concentration gradients of element 2 on the fluxes of element 1 and element 1 on element 2, respectively. For semi-infinite diffusion couples, the initial and boundary conditions are

$$C_i(-x,0)=C_i(-\infty,t)=C_i^- \ (i=1,2)$$
$$C_i(x,0)=C_i(+\infty,t)=C_i^+ \ (i=1,2) \qquad (2)$$

Kirkaldy et al. [14] have shown that Eq. (1) can be solved by an extension of the Boltzmann-Matano method into a ternary one:

$$\int_{C_1^-}^{C_1} xdC_1 = -2t(\tilde{D}_{11}^3 \frac{\partial C_1}{\partial x} + \tilde{D}_{12}^3 \frac{\partial C_2}{\partial x})$$
$$\int_{C_2^-}^{C_2} xdC_2 = -2t(\tilde{D}_{21}^3 \frac{\partial C_1}{\partial x} + \tilde{D}_{22}^3 \frac{\partial C_2}{\partial x}) \qquad (3)$$

Assuming that the volume change is negligible, the position of the Matano plane should be the same for concentration profiles of solutes 1 and 2 theoretically. In order to avoid the effect of the uncertainties of Matano plane on the calculated diffusivity, Whittle and Green [13] have suggested to introduce the normalized concentration parameter

$$Y_i = (C_i - C_i^-)/(C_i^+ - C_i^-) \ (i=1,2) \qquad (4)$$

Then the ternary interdiffusion coefficients can be determined by solving the following equations:

$$\tilde{D}_{11}^3 + \tilde{D}_{12}^3 \frac{dC_2}{dC_1} = \frac{1}{2t}\frac{dx}{dY_1}[(1-Y_1)\int_{-\infty}^x Y_1 \cdot dx +$$
$$+ Y_1 \int_x^{+\infty}(1-Y_1)\cdot dx] \qquad (5)$$
$$\tilde{D}_{22}^3 + \tilde{D}_{21}^3 \frac{dC_1}{dC_2} = \frac{1}{2t}\frac{dx}{dY_2}[(1-Y_2)\int_{-\infty}^x Y_2 \cdot dx +$$
$$+ Y_2 \int_x^{+\infty}(1-Y_2)\cdot dx]$$

The four interdiffusion coefficients in Eqs. (5) are evaluated at the intersection of the diffusion paths from two diffusion couples.

The standard deviation of the interdiffusivities extracted in the current work is evaluated using the scientific method proposed by Lechelle et al. [15], who considered the error propagation via the following function:

$$u(f(A,B...)) = \sqrt{\sum_{\alpha=A,B...} \left(\frac{\partial f}{\partial \alpha}\right)^2 (u(\alpha))^2} \qquad (6)$$

Here, A and B are the correlation quantities of function f, while $u(\alpha)$ $(\alpha = A, B...)$ is the uncertainty in the measurements of variable a like concentration.

4. Results and discussion

4.1 The measured concentration profiles and fitting functions

Considering that all the 6 diffusion couples are in the same fcc single-phase region, one typical microstructure of the diffusion zone is given in Fig. 1, which shows the backscattered electron image (BEI) of couple C5 (Cu/Cu–4.06Ni–2.83Sn) annealed at 1073 K for 36 h. The concentration profiles of each component in all the diffusion couples (symbols) measured by EPMA are presented in Figs. 2 and 3. Data processing of the original EPMA data is required especially when the number of experimental points is limited and the scattered data cannot guarantee the reliability of calculated diffusivities. Different fitting functions are adopted to treat the experimental profiles and generate the smooth concentration profiles relative to the distance. Some typically and successfully utilized fitting functions will be presented here. The symbols C and x in the following expressions are the concentration and diffusion distance, respectively.

For symmetrical concentration profiles, the Boltzmann function is the most widely used fitting function, which is expressed as [16-19]:

$$C(x) = \frac{A_1 - A_2}{1 + e^{(x-x_0) \cdot dx}} + A_2 \qquad (7)$$
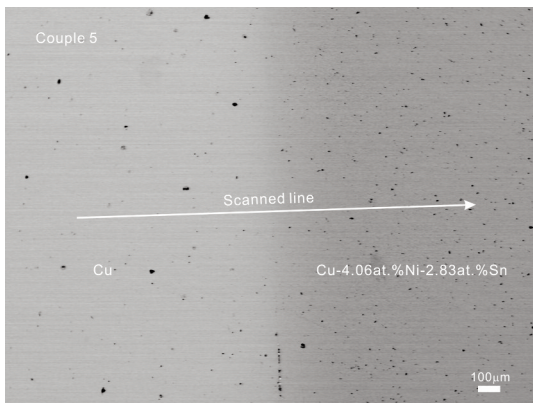
Figure 1. Backscattered electron image of the microstructure of C5 (Cu/Cu–4.06Ni–2.83Sn) after annealing at 1073 K for 36 h.
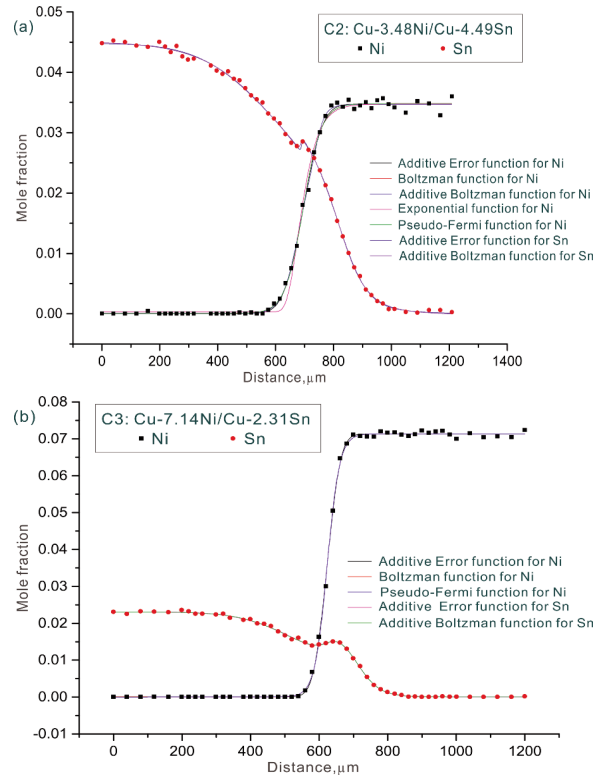
Figure 2. Measured and fitted concentration profiles for (a) C2 (Cu–3.48Ni/Cu–4.49Sn) and (b) C3 (Cu–7.14Ni/Cu–2.31Sn) after annealing at 1073 K for 36 h. Symbols are from the experimental measurements, while solid lines are the fitted concentration profiles.

where A_1, A_2, x_0 and dx are the parameters to be fitted. x_0 presents the position of Matano plane.

For complex asymmetrical concentration profile as displayed in the present work of Sn, the additive Boltzmann function is a good choice:

$$C(x) = A_1 + \frac{A_2}{1 + e^{(x-A_3)/A_4}} + \frac{A_5}{1 + e^{(x-A_6)/A_7}} + \frac{A_8}{1 + e^{(x-A_9)/A_{10}}} + ... \qquad (8)$$

where A_i(i=1,2,3,...) are the parameters to be fitted. It is preferable to use less parameter if the fitting results from different selections of parameters are similar to each other.

Exponential function is employed to describe the slightly asymmetric diffusion behaviors [20, 21]:

$$C(x) = p_1 \exp(-\exp(p_2 - p_3 x)) + p_4 \qquad (9)$$

where p_i(i=1~4) are the parameters to be fitted.

Cubic function is found to be more suitable for the experimental data showing the phenomena of up-hill diffusion [20, 21]:

$$C(x) = \frac{p_1 + p_3 x + p_5 x^2 + p_7 x^3}{1 + p_2 x + p_4 x^2 + p_6 x^3} \qquad (10)$$

in which $p_i(i=1\sim4)$ are the parameters to be fitted.
Pseudo-Fermi type function is adopted to reproduce the highly asymmetric concentration profile [22]:

$$C(x) = \frac{p_1 - p_2 x}{1 + \exp\left(\dfrac{x + p_3}{p_4}\right)} + p_5 \qquad (11)$$

where $p_i(i=1\sim5)$ are the parameters to be fitted.
Additive Error function can depict both simple and complicated, symmetric and asymmetric concentration profiles [23]:

$$C(x) = p_1 + p_2\mathrm{erfc}(p_3 x + p_4) + \\ + p_5\mathrm{erfc}(p_6 x + p_7) + p_8\mathrm{erfc}(p_9 x + p_{10}) \qquad (12)$$

where $p_i(i=1\sim10)$ are the parameters to be fitted. It should be noted that it may result in unexpected concentration gradient and then lead to much uncertainties.

A large number of other fitting functions have been proposed, such as Fourier series function [24], Cubic Spline function [25], the four functions proposed in Ref. [26], the Polynomial function [27] and function proposed in Ref. [15]. There is always an inconsistency regarding to the option of fitting functions. Here C2/C5 and C2/C3 diffusion couples

are chosen as examples to illustrate the effect of different fitting functions on the computed diffusivities.

According to the simple variable method, only the type of fitting functions for Ni of C2 in diffusion couples C2/C5 is changed here. The experimental data for Sn of C2 are fitted by additive Boltzmann function, while those for Ni and Sn of C5 are fitted by Boltzmann function. The measured data for Ni of C2 without up-hill diffusion can be described by additive Error, Boltzmann, additive Boltzmann, Exponential and Pseudo-Fermi type functions, which are named as types 1 to 5, respectively. All these fitting functions of C2 are also superimposed with the measured data, as shown in Fig. 2(a). The Residual Sum of Squares of different fitting functions for Ni are listed in Table 2. Subsequently these functions are employed to calculate the interdiffusivities and their uncertainties of fcc Cu–Ni–Sn alloys. The obtained interdiffusivities together with their deviations are exhibited in Table 2 and Fig. 4. The comparison among the calculated interdiffusivities shows a general agreement with each other, especially for the main diffusion coefficients. The interdiffusivities extracted from the Exponential function (type 4) have large uncertainties, and these can be explained by the
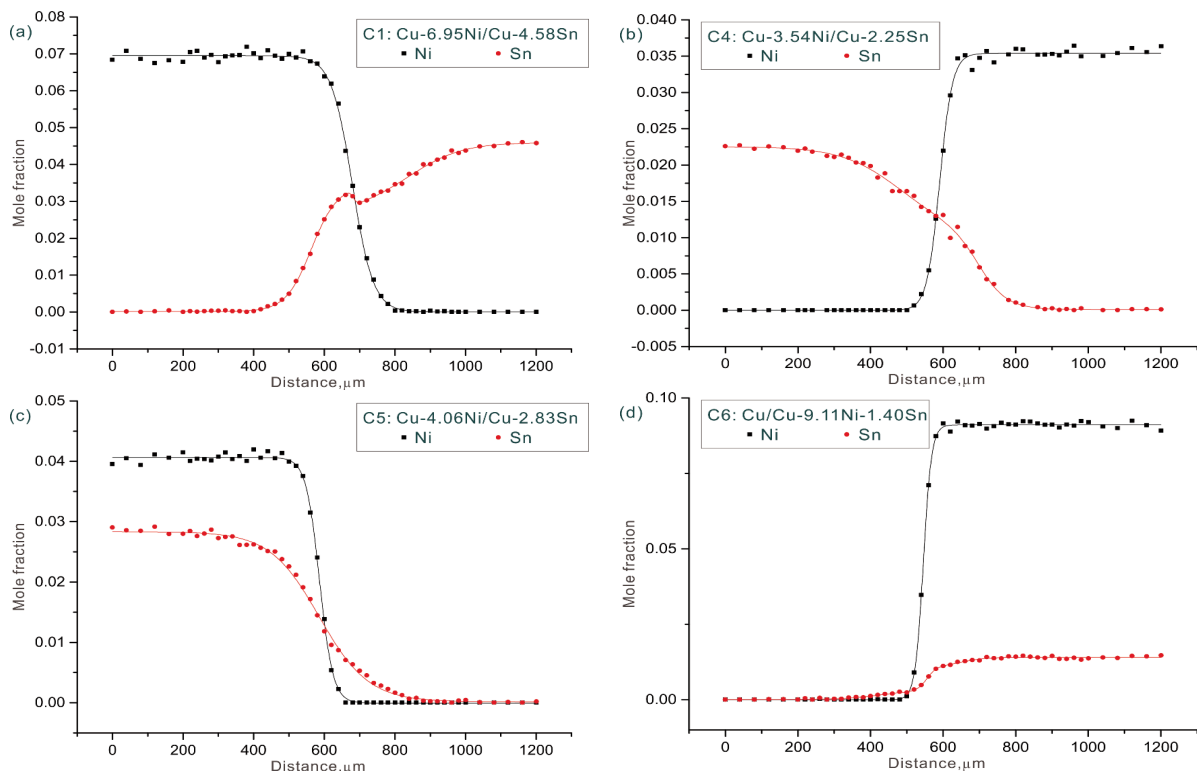
Figure 3. Measured and fitted concentration profiles for (a) C1 (Cu–6.95Ni/Cu–4.58Sn), (b) C4 (Cu–3.54Ni/Cu–2.25Sn), (c) C5 (Cu/Cu–4.06Ni–2.83Sn) and (d) C6 (Cu/Cu–9.11Ni–1.40Sn) after annealing at 1073 K for 36 h. Symbols are from the experimental measurements, while solid lines are the fitted concentration profiles. The fitting function for Ni in (a)-(d) is Boltzmann function, and for Sn in (a)-(c) is Boltzmann function and in (d) is additive Boltzmann function.

inconsistence between the measured and fitted profiles as displayed in Fig. 2 (a). And this Residual Sum of Squares in type 4 also means a poor fitting. Besides, it can be found that type 3 has the smallest Residual Sum of Squares which demonstrates the best fitting composition profile. However, type 3 has a large error and thus is not recommended here. Since the original data is scattered and the best fitting will result in unexpected concentration gradient and make the result worse. Therefore, the Residual Sum of Squares is not taken into account in next discussion. One also notes that the position deviation of different fitting function for intersection point is so small that this uncertainties can be negligible and thus not taken into account in this work.

The Sn concentration profiles of C2 and C3 show a complex feature including a change of sign for the slope of the tangent line which is caused by the accumulation of Sn. The diffusion distance of Sn is larger than that of Ni, which illustrates that Sn diffuses faster than Ni. On the other hand, Ni can effectively impede the diffusion of Sn. Therefore, Sn moves fast from Cu–Sn binary alloy, then accumulates in the interface of Cu–Ni binary alloy and forms this slope. In order to reproduce this slope in Sn concentration profile, the additive Boltzmann and additive Error functions are used. Additive Boltzmann and additive Error functions for Sn in both C2 and C3 are employed in types 1 to 4 and 5 to 8, respectively. Considering the unsatisfactory fitting of Exponential function, the additive Error, Boltzmann, additive Boltzmann and Pseudo-Fermi type functions are utilized for Ni. Types 1 to 4 represent additive Error, Boltzmann, additive Boltzmann and Pseudo-Fermi type

functions for Ni in C2 and additive Error, Boltzmann, Boltzmann and Pseudo-Fermi type functions in C3, respectively. Types 5 to 8 correspond to the same fitting functions for Ni as types 1 to 4, respectively. The above fitting functions are appended in Fig. 2. The corresponding calculated interdiffusivities along with their uncertainties are presented in Table 3 and Fig. 5. A general agreement can be found among these extracted results. In addition, the large error is found in types 1, 3 and 5 to 8, especially regarding the cross interdiffusion coefficients. Therefore, types 1, 3 and 5 to 8 are
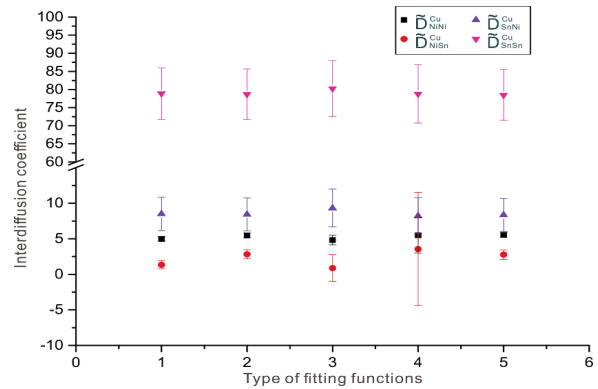
Figure 4. *Diffusion coefficients of diffusion couples C2/C5 with different fitting functions applied to measured concentration profiles. The fitting function for Sn of C2 is additive Boltzmann function, for Ni and Sn of C5 are Boltzmann functions, and for Ni of C2 are additive Error, Boltzmann, additive Boltzmann, Exponential and Pseudo-Fermi type functions, which response to types 1 to 5, respectively.*

Table 2. *Diffusion coefficients of diffusion couples C2/C5 with different fitting functions applied to measured concentration profiles.*

Type	Fitting functions [a]				Composition (at.%)		Interdiffusion coefficient ($\times 10^{-15}$ m^{2}s^{-1}) [b]			
	C2-Ni (RS) [c]	C2-Sn	C5-Ni	C5-Sn	Ni	Sn	$\tilde{D}_{NiNi}^{Cu}$ (SD)	$\tilde{D}_{NiSn}^{Cu}$ (SD)	$\tilde{D}_{SnNi}^{Cu}$ (SD)	$\tilde{D}_{SnSn}^{Cu}$ (SD)
C2/C5-1	additive Err (1.7)	additive Bol	Bol	Bol	3.4	1.72	4.98 (± 0.30)	1.35 (± 0.55)	8.50 (± 2.36)	78.87 (± 7.14)
C2/C5-2	Bol (1.9)	additive Bol	Bol	Bol	3.37	1.72	5.47 (± 0.32)	2.83 (± 0.63)	8.43 (± 2.31)	78.67 (± 7.00)
C2/C5-3	additive Bol (1.6)	additive Bol	Bol	Bol	3.42	1.74	4.82 (± 0.68)	0.88 (± 1.88)	9.31 (± 2.66)	80.24 (± 7.75)
C2/C5-4	Exp (4.6)	additive Bol	Bol	Bol	3.35	1.72	5.48 (± 2.51)	3.55 (± 7.97)	8.22 (± 2.56)	78.79 (± 8.08)
C2/C5-5	Pse (1.9)	additive Bol	Bol	Bol	3.37	1.72	5.55 (± 0.33)	2.76 (± 0.66)	8.34 (± 2.31)	78.47 (± 6.99)

[a] Err = additive Error function; Bol = Boltzmann function; Additive Bol = additive Boltzmann function; Exp = Exponential function; Pse =Pseudo-Fermi type function.s; [b] SD = standard deviation, which is evaluated by a scientific method considering the error propagation. [c] RS = Residual Sum of Squares, (´10⁵).

not considered here. The additive type functions with abundant parameters are easy to cause large error. Considering the popularity and smaller uncertainties in these two examples, Boltzmann function for Ni and additive Boltzmann function for Sn are suggested to be the fitting functions of concentration profiles.
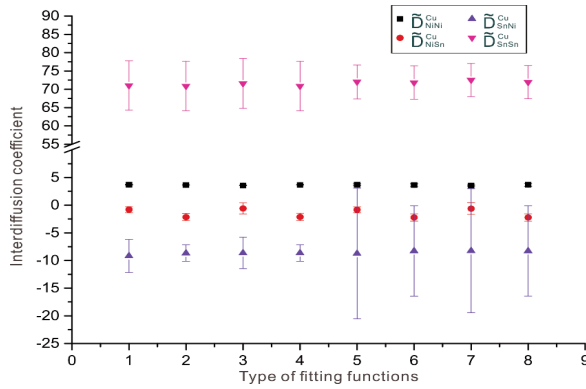
Figure 5. *Diffusion coefficients of diffusion couples C2/C3 with different fitting functions applied to measured concentration profiles. Additive Boltzmann and additive Error functions for Sn in both C2 and C3 are employed in types 1 to 4 and 5 to 8, respectively. Types 1 to 4 represent additive Error, Boltzmann, additive Boltzmann and Pseudo-Fermi type functions for Ni in C2 and additive Error, Boltzmann, Boltzmann and Pseudo-Fermi type functions in C3, respectively. The types 5 to 8 are with the same fitting function for Ni to the types 1 to 4, respectively.*

4.2 Determination of ternary interdiffusion coefficients

Based on the investigation of fitting functions in Section 4.1, the Boltzmann function is recommended firstly to fit the measured concentration profiles. For the complex measured ones, the additive Boltzmann function is employed. All the fitting functions are compared with their measured data as shown in Figs. 2 and 3. Fig. 6 is the isothermal section of Cu-rich Cu–Ni–Sn system at 1073 K [28], together with the measured and fitted diffusion paths of the six diffusion couples in this work. The obtained ternary interdiffusion coefficients at the 8 intersection points of the diffusion couples together with the standard deviation are listed in Table 4. It can be found that the values of the main interdiffusion coefficients $\tilde{D}_{SnSn}^{Cu}$ are almost larger than $\tilde{D}_{NiNi}^{Cu}$ by one order of magnitude, which are coincided with the observation of the measured concentration profiles. Besides, the cross interdiffusivities $\tilde{D}_{SnNi}^{Cu}$ are negative and it demonstrates that the concentration gradient of Ni will impede the diffusion of Sn.

The reliability of the currently obtained ternary interdiffusivities in fcc Cu-rich Cu–Ni–Sn alloys is validated by the thermodynamic stability, which is defined as [29]:

$$\tilde{D}_{NiNi}^{Cu} + \tilde{D}_{SnSn}^{Cu} > 0$$
$$\tilde{D}_{NiNi}^{Cu} \cdot \tilde{D}_{SnSn}^{Cu} - \tilde{D}_{NiSn}^{Cu} \cdot \tilde{D}_{SnNi}^{Cu} \geq 0 \qquad (13)$$
$$(\tilde{D}_{NiNi}^{Cu} - \tilde{D}_{SnSn}^{Cu})^2 + 4 \cdot \tilde{D}_{NiSn}^{Cu} \cdot \tilde{D}_{SnNi}^{Cu} \geq 0$$

Table 3. *Diffusion coefficients of diffusion couples C2/C3 [d] with different fitting functions applied to measured concentration profiles.*

Type	Fitting functions [e]				Interdiffusion coefficient ($\times 10^{-15} m^2 s^{-1}$) [f]			
	C2-Ni	C2-Sn	C3-Ni	C3-Sn	$\tilde{D}_{NiNi}^{Cu}$ (SD)	$\tilde{D}_{NiSn}^{Cu}$ (SD)	$\tilde{D}_{SnNi}^{Cu}$ (SD)	$\tilde{D}_{SnSn}^{Cu}$ (SD)
C2/C3-1	additive Err	additive Bol	additive Err	additive Bol	3.71 ($\pm$ 0.04)	-0.80 ($\pm$ 0.54)	-9.17 ($\pm$ 2.98)	71.03 ($\pm$ 6.78)
C2/C3-2	Bol	additive Bol	Bol	additive Bol	3.64 ($\pm$ 0.05)	-2.14 ($\pm$ 0.64)	-8.66 ($\pm$ 1.48)	70.87 ($\pm$ 6.76)
C2/C3-3	additive Bol	additive Bol	Bol	additive Bol	3.58 ($\pm$ 0.04)	-0.58 ($\pm$ 1.00)	-8.64 ($\pm$ 2.83)	71.58 ($\pm$ 6.82)
C2/C3-4	Pse	additive Bol	Pse	additive Bol	3.68 ($\pm$ 0.05)	-2.13 ($\pm$ 0.66)	-8.65 ($\pm$ 1.48)	70.87 ($\pm$ 6.76)
C2/C3-5	additive Err	additive Err	additive Err	additive Err	3.71 ($\pm$ 0.14)	-0.84 ($\pm$ 0.56)	-8.75 ($\pm$ 11.81)	71.99 ($\pm$ 4.63)
C2/C3-6	Bol	additive Err	Bol	additive Err	3.63 ($\pm$ 0.25)	-2.23 ($\pm$ 0.66)	-8.28 ($\pm$ 8.16)	71.83 ($\pm$ 4.56)
C2/C3-7	additive Bol	additive Err	Bol	additive Err	3.57 ($\pm$ 0.10)	-0.61 ($\pm$ 1.04)	-8.24 ($\pm$ 11.2)	72.53 ($\pm$ 4.53)
C2/C3-8	Pse	additive Err	Pse	additive Err	3.69 ($\pm$ 0.25)	-2.23 ($\pm$ 0.69)	-8.27 ($\pm$ 8.16)	71.91 ($\pm$ 4.51)

[d] *The common composition of C2/C3 diffusion couples is 3.41 at.% Ni and 1.47 at.% Sn.* [e] *Err = additive Error function; Bol = Boltzmann function; additive Bol = additive Boltzmann function; Pse = Pseudo-Fermi type function.* [f] *SD = standard deviation, which is evaluated by a scientific method considering the error propagation.*

Table 4. *Diffusion coefficients in Cu-rich fcc Cu–Ni–Sn alloys at 1073 K obtained in this work.*

Diffusion couple	Composition (at.%)		Interdiffusion coefficient ($\times 10^{-15}$m^{2}s^{-1}) [g]			
	Ni	Sn	$\tilde{D}_{NiNi}^{Cu}$ (SD)	$\tilde{D}_{NiSn}^{Cu}$ (SD)	$\tilde{D}_{SnNi}^{Cu}$ (SD)	$\tilde{D}_{SnSn}^{Cu}$ (SD)
C1/C6	6.91	0.75	1.59 (± 0.17)	-1.28 (± 1.56)	-2.24 (± 0.85)	32.15 (± 7.61)
C2/C5	3.37	1.72	5.47 (± 0.32)	-2.83 (± 0.63)	-8.43 (± 2.31)	78.67 (± 7.00)
C2/C6	3.48	0.48	1.43 (± 0.12)	-0.57 (± 0.96)	-2.36 (± 1.98)	57.33 (± 14.37)
C2/C3	3.41	1.47	3.64 (± 0.05)	-2.14 (± 0.64)	-8.66 (± 1.48)	70.87 (± 6.76)
C3/C5	2	1.42	3.81 (± 0.27)	0.71 (± 0.40)	-10.72 (± 8.57)	108.57 (± 32.94)
C3/C6	7.1	0.77	1.66 (± 0.07)	-0.86 (± 0.43)	-2.25 (± 0.82)	30.68 (± 5.23)
C4/C5	1.4	1.29	3.57 (± 0.05)	2.17 (± 0.29)	-5.61 (± 1.01)	79.19 (± 4.87)
C4/C6	3.53	0.48	1.42 (± 0.05)	-0.38 (± 0.81)	-1.95 (± 1.70)	46.92 (± 8.12)

[g] *SD = standard deviation, which is evaluated by a scientific method considering the error propagation.*
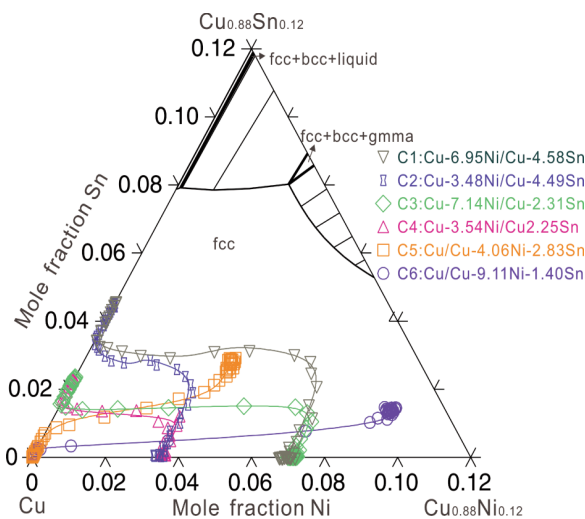
Figure 6. *Isothermal section of Cu-rich Cu–Ni–Sn system at 1073 K [28], together with the measured and fitted diffusion paths of the six diffusion couples in this work.*

All the current interdiffusion coefficients satisfy the above thermodynamic constraints which purport thermodynamically stable. Therefore, it can be concluded that the currently obtained ternary interdiffusion coefficients are reliable.

5. Conclusions

Based on six groups of bulk diffusion couples, the ternary interdiffusion coefficients in fcc Cu–Ni–Sn alloys at 1073 K were determined by means of EPMA technique coupled with the Whittle and Green method. The different fitting functions employed to the measured concentration profiles are utilized to obtain the interdiffusion coefficients of fcc Cu–Ni–Sn alloys. The comparison among the extracted interdiffusion coefficients with different fitting functions shows that Boltzmann and additive Boltzmann functions are more suitable for fcc Cu–Ni–Sn alloys due to the small uncertainties. Using Boltzmann and the additive Boltzmann functions to fit the measured concentration profile, the interdiffusivities in Cu-rich fcc Cu–Ni–Sn alloys at 1073 K are obtained and validated by thermodynamic constraints. The Boltzmann and additive Boltzmann functions are suggested to fit the measured concentration profiles in other ternary systems.

References

[1] B.Q. Ma, J.Q. Li, Z.J. Peng, G.C. Zhang, Journal of Alloys and Compounds, 535 (2012) 95-101.
[2] J.T. Plewes, Metall. Mater. Trans. A, 6 (3) (1975) 537.
[3] J.C. Zhao, M.R. Notis, Acta Materialia, 46 (12) (1998) 4203-4218.
[4] M. Abtew, G. Selvaduray, Mat. Sci. Eng. R., 27 (5–6) (2000) 95-141.
[5] K. Zeng, K.N. Tu, Mat. Sci. Eng. R., 38 (2) (2002) 55-105.
[6] Y. Li, C.P. Wong, Mat. Sci. Eng. R., 51 (1–3) (2006) 1-35.
[7] B.Ç. P. Topuz, O. Akar, J. Min. Metall. Sect. B-Metall., 52 (1) (2016) 63-68.

[8]   J. Wang, C. Leinenbach, H.S. Liu, L.B. Liu, M. Roth, Z.P. Jin, J. Phase Equilib. Diff., 31 (1) (2010) 28-33.

[9]   M.K. T. Takahashi, Shindo Gijutsu Kenkyu Kaishi 33 (1994) 88-101.

[10] G.H. Cheng, M.A. Dayananda, Metall. Trans., 10A (1979) 1415-1419.

[11] Y.H. Sohn, M.A. Dayananda, Metall. Mater. Trans. A, 33 (11) (2002) 3375-3392.

[12] Y. Du, B. Sundman, J. Phase Equilib. Diffus., (2017) Ahead of Print.

[13] D.P. Whittle, A. Green, Scr. Mater., 8 (1974) 883-884.

[14] J.S. Kirkaldy, J.E. Lane, G.R. Mason, Can. J. Phys. , 33 (1963) 2174-2186.

[15] J. Lechelle, S. Noyau, L. Aufore, A. Arredondo, E. Audubert, Diffus. Fundam. Org., 17 (2012) 1-39.

[16] J. Chen, L. Zhang, J. Zhong, W. Chen, Y. Du, Journal of Alloys and Compounds, 688, Part A (2016) 320-328.

[17] J. Chen, J. Xiao, L. Zhang, Y. Du, Journal of Alloys and Compounds, 657 (2016) 457-463.

[18] R. Wang, L. Zhang, Z. Lu, Y. Du, Z. Jin, D. Živković, J. Phase Equilib. Diff., 36 (5) (2015) 510-517.

[19] J. Li, W. Chen, D. Liu, W. Sun, L. Zhang, Y. Du, H. Xu, J. Phase Equilib. Diff., 34 (6) (2013) 484-492.

[20] D. Liu, L. Zhang, Y. Du, H. Xu, Z. Jin, Journal of Alloys and Compounds, 566 (2013) 156-163.

[21] K. Cheng, D. Liu, L. Zhang, Y. Du, S. Liu, C. Tang, Journal of Alloys and Compounds, 579 (2013) 124-131.

[22] E. Rabkin, V.N. Semenov, A. Winkler, Acta Materialia, 50 (12) (2002) 3229-3239.

[23] D. Kuang, D. Liu, W. Chen, Z. Lu, L. Zhang, Y. Du, Z. Jin, C. Tang, Int. J. Mater. Res., 107 (7) (2016) 597-604.

[24] K.W. Moon, C.E. Campbell, M.E. Williams, W.J. Boettinger, J. Phase Equilib. Diff., 37 (4) (2016) 402-415.

[25] Q. Zhang, J.-C. Zhao, Intermetallics, 34 (2013) 132-141.

[26] S.K. Kailasam, J.C. Lacombe, M.E. Glicksman, Metall. Mater. Trans. A, 30 (10) (1999) 2605-2610.

[27] B. Messerschmidt, B.L. McIntyre, S.N. Houde-Walter, R.R. Andre, C.H. Hsieb, Optical Materials, 7 (4) (1997) 165-171.

[28] J. Miettinen, Calphad, 27 (3) (2003) 309-318.

[29] L. Onsager, Ann. N. Y. Acad. Sci., 46 (5) (1945) 241-265.